Indicators for the Damage Evolution at Intermediate Temperature Under Air of a SiC/[Si-B-C] Composite Subjected to Cyclic and Static Loading

Elie Racle, Nathalie Godin, Pascal Reynaud, Mohamed R'Mili, Gilbert Fantozzi, Lionel Marcin, Florent Bouillon, Myriam Kaminski

INDICATORS FOR THE DAMAGE EVOLUTION AT INTERMEDIATE TEMPERATURE UNDER AIR OF A SIC/[SI-B-C] COMPOSITE SUBJECTED TO CYCLIC AND STATIC LOADING

Elie Racle[1,2], Nathalie Godin[1], Pascal Reynaud[1], Mohamed R'Mili[1], Gilbert Fantozzi[1], Lionel Marcin[2], Florent Bouillon[3] and Myriam Kaminski[4]
[1] MATEIS, INSA-Lyon, F-69621 Villeurbanne, France
[2] SNECMA – Groupe SAFRAN, rond-point René Raveau, F- 77550 Moissy Cramayel, France
[3] HERAKLES - Groupe SAFRAN, Les Cinq Chemins, F- 33185 Le Haillan, France
[4] ONERA, 29 avenue de la Division Leclerc, F- 92322 Chatillon, France

ABSTRACT

The low density and the high tensile strength of Ceramic Matrix Composites (CMC) make them a good technical solution to design aeronautical structural components. To fully understand damage mechanisms and be able to design components, its behavior has to be analyzed during fatigue tests. The aim of the present study is to compare behavior of this composite under static and cyclic loading. Tests are realized under the same conditions of temperature and maximal load levels in order to determine the effects of cycles on the sequence of damage mechanisms. Hence the evolution of mechanical parameters is analyzed. Nevertheless the complexity of mechanisms and duration of tests make the use of complementary damage indicators necessary. Different approaches based on acoustic emission can be taken into consideration in order to quantify damage along the tests. In this case the analysis of acoustical energy is studied by comparing to the evolution of strain energy. This method enables to point out different damage levels during tests.

INTRODUCTION

To optimize design of parts, the mechanical behavior has to be fully understood. The aim of the study consists in analyzing and comparing material behavior under cyclic and static fatigue loadings, at the same temperature and under air, to determine effects of a cyclic loading on damage and lifetime. CMCs seems to be promising material for aeronautical applications, even if its constituent materials are brittle, the strain at failure is rather high due to considerable matrix cracking and cracks deflection at interfaces[1]. However, these materials behavior is affected by oxidation of interphases and fibers and the ultimate failure is governed by slow crack growth in fibers[2]. Self-healing material has been developed to protect fibers against oxidation, which increased largely the lifetime of material. Nevertheless, under air and for temperature above 550°C, self-healing is not significant enough to fully protect the material. This is why it is important to understand the material behavior for those temperatures.

As specified above, the lifetimes under these types of loadings are rather long which makes it hard to realize tests on laboratory equipment. This kind of studies needs to be done with a limited number of tests, thus the use of different techniques to monitor the damage in real time is mandatory. Acoustic emission (AE) appears to be a good candidate in this case. It consists of recording transient elastic waves on the material created by damage mechanisms. There are several studies referring to this kind of method for different types of CMCs under tensile

tests[3,4,5]. For fatigue tests, damage can be analyzed from different points of view, first by linking each acoustical event to the damage mechanism which generated it[6]. This process needs clustering algorithms[7]. Another approach consists in considering the evolution of released energy[8-10]. It is generally accepted that the energy of an AE signal is related to the energy released by the source. Consequently, AE energy gives information about material damage; it is then possible to point out precursory elements to ultimate failure or to simulate AE energy evolution with a power law to determine lifetime.

In the current study, the global AE is analyzed and compared to the mechanical energy during cyclic and static fatigue tests. This process is based on studies realized by Minak[11,12] on organic matrix composites. The goal of this process is to determine new damage markers for CMCs.

EXPERIMENTAL

The material is composed of Nicalon SiC fibers coated with PyC and a self-healing [Si-B-C]. The fibers reinforcement is composed of several layers of 2D satin fabrics linked together by strands of fibers in the third direction. In this study all the specimens have a dog-bone shape with a thickness of 4 mm and a gauge section of 60 mm x 16 mm.

Tests are realized at a temperature of 450°C. This temperature is critical for the material since SiC can be degraded by oxidation without any self-healing effect. Three different types of tests are performed: tensile tests, static fatigue tests and cyclic fatigue tests. Cyclic fatigue tests are made on hydraulic tensile test machine whereas tensile and static tensile tests are made on a pneumatic tensile machine which has been designed to allow a long constant load. Strain is measured using extensometer. In the case of static fatigue tests, in order to determine what stress level creates damage on the material because of oxidation, the imposed stress increases every T_i (time for 18% of N_f, number of cycles to failure) of 6 % of tensile strength. At the same time cyclic fatigue tests are realized with imposed stress oscillating at a frequency of 2 Hz between 0 and an incremental maximum value which is increasing of 6 % every 18% of N_f (Figure 1)

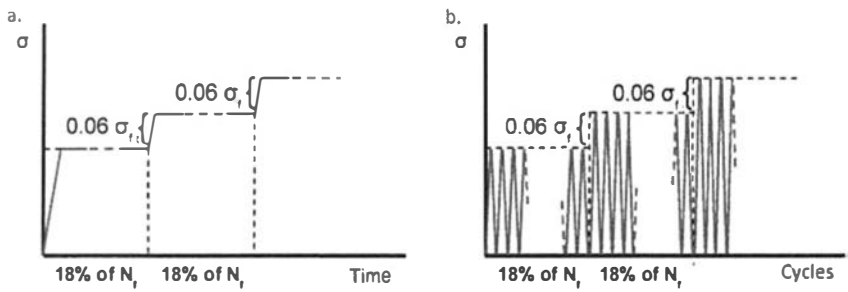

Figure 1. Applied stress for a. Static fatigue test b. Cyclic fatigue test

ACOUSTIC EMISSION

Acquisition System

Two piezoelectric sensors (Micro80, Mistras Group) are maintained on the specimen surface. Medium viscosity vacuum grease is used to ensure a good coupling between the specimen and sensors. Each sensor is connected to the data acquisition system (PCI2, Mistras Group) via a preamplifier with a 40 dB gain and 20-1200 kHz bandwidth (Mistras Group). For each detected signal, with an acquisition threshold of 45 dB on the pneumatic tensile machine and 55 dB on the hydraulic tensile machine, the data acquisition system records waveform descriptors such as amplitude or duration and mechanical information (stress, strain).

Location of AE sources

During tests, AE is recorded with 2 piezoelectric sensors, one on each side of the reduced section (Figure 2). The position of a detected source can be determined linearly knowing the wave velocity in the material using the formula described in eq. (1)

$$x = \frac{1}{2} v(t_{sens2} - t_{sens1}) \quad (1)$$

where v is the wave velocity in the material, t_{sens1} and t_{sens2} respectively the arrival times of signals generated by the same source on sensor 1 and sensor 2. The velocity is determined simulating an AE source with the Hsu-Nielsen pencil lead breakage procedure; it depends on sensor setup and the detection threshold. It is evaluated to 8500 m/s on the pneumatic setup and 7500 m/s on the hydraulic setup. The velocity also evaluates when the material is being damaged. It has been seen that v could be corrected using the evolution of the secant elastic modulus[4] as shown in eq. (2)

$$v(t) = v_0 . \sqrt{\frac{E(t)}{E_0}} \quad (2)$$

where E(t) is the secant elastic modulus at time t and E_0 the Young's Modulus of the material. The velocity is thus evaluated for each cycle during cyclic fatigue tests. Unloading/loading cycles are realized regularly for tensile and static fatigue tests to estimate evolution of secant elastic modulus. It allows to consider only events which are emitted from the reduced section, and to eliminate noise from the equipment. In the following, AE events will be considered if the distance between its source and the middle of the specimen is less than 30 mm.

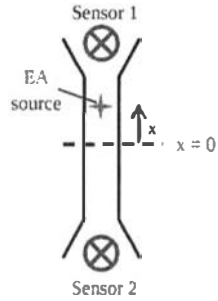

Figure 2. AE setup on a composite specimen

Acoustic energy

Since the acoustic energy is related to material damage, cumulated acoustic energy progression during a test can be considered as an indicator of damage evolution. It is obtained by summing the energy of each event localized in the gauge section of the specimen. Nevertheless for an event, different energy values can be chosen depending on the sensor. These values also depend on the propagation on the material as seen in eq. 3.

$$U_{sens1} = U_{source} \cdot A_{sens1} \cdot e^{-B\left(\frac{L}{2}+x\right)} \quad (3.a)$$

$$U_{sens2} = U_{source} \cdot A_{sens2} \cdot e^{-B\left(\frac{L}{2}-x\right)} \quad (3.b)$$

with x defined in Figure 2, L the distance between the 2 sensors, U_{source} the acoustic energy released by the source, A_{sensi} the coupling effects between sensor i and the material and B the attenuation factor. This is why for each localized source, the equivalent energy is U_e considered (eq. 4)

$$U_e = \sqrt{U_{sens1} \cdot U_{sens2}} = U_{source} \cdot \sqrt{A_{sens1} \cdot A_{sens2}} \cdot e^{-\frac{B.L}{2}} \quad (4)$$

This makes that U_{se} is not function of the location of the source position.

To evaluate the evolution of acoustic energy, the R_{ae} rate can be calculated using eq. 5

$$R_{ae} = \frac{\Delta U_e}{\Delta t} \quad (5)$$

Where $Tu_{e.}$ is the cumulated energy of N signals, and Δt the time between the first and the last signals of the N signals. This rate is calculated every n signals. N is chosen depending on the acoustic activity (N~1% of number of signals). It has to be high enough to get a smooth curve. n is usually chosen weaker than N but close enough to have enough accuracy (n~0.90-0.95.N).

Sentry function

Sentry function has been defined by Minak in order to compare mechanical evolution during a test to acoustical activity. Variations of the function can show different levels of damage in the composite. Sentry function is defined in eq. (6)

$$f = \ln(\frac{U_s}{U_{ae}}) \quad (6)$$

where U_s is strain energy and U_{ae} the cumulated acoustical energy. f can be function of time or strain. It is defined as soon as the first acoustical event is recorded. Strain energy is calculated measuring the area under the force-displacement curve (Figure 3). To determine only the effects of tension, unloading/loading loads are not taken into consideration. The function is calculated every k acoustic sources (k~0.1% of number of signals). This enables not to consider singular event and to obtain a smother curve. It could be calculated for a fixed strain value but that would erase variation when strain remains constant during fatigue tests.

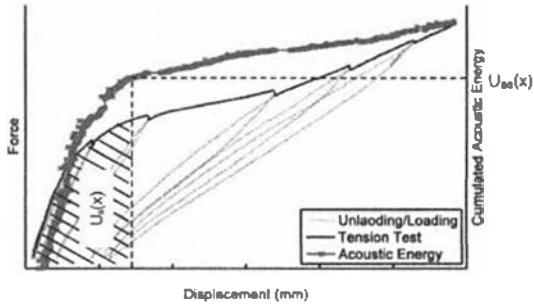

Figure 3. Calculation of the Sentry Function, determination of strain energy and acoustic energy

RESULTS AND DISCUSSION

Mechanical Behavior in Static and Cyclic Fatigue

To compare the results of static and cyclic fatigue tests, the behavior of the material during a tensile test is used as a reference. Thereafter, σ_R and ε_R will respectively represent ultimate tensile strength and strain at failure. The behavior of the material can be decomposed in 4 phases (Figure 4). It has first a linear behavior, until the ultimate strength of matrix. During a second phase, the matrix cracks until saturation. While matrix cracking almost reaches its saturation, interfaces debonding creates a large increase of the strain. At the end, the whole stress is carried by the fibers, until the failure of the material. The elastic modulus can be determined along the test by realizing unloading/loading cycles. It appears that it decreases as far as the matrix is cracking and tends toward an asymptotic value which corresponds to the product $Ef.vf$ where E_f is the Young's modulus of fibers and v_f the fibers volume fraction.

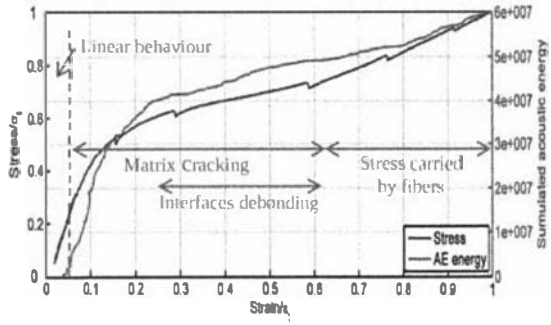

Figure 4. Stress-strain curve & cumulated acoustic energy vs. strain during a tensile test at 450°C

Results of fatigue test are summarized in the Table 1. Static fatigue tests were conducted with a first level of loading slightly higher than the elastic limit of the material (18% of tensile strength). Two cyclic fatigue tests were realized with the same maximal stress during stage 1. A third test was done with an extra stage (stage 0) where the maximal stress was included in the linear part of the material. This third test is presented here since it gives a larger vision of the effects of a cyclic loading and it is representative of the material behavior for this kind of tests.

Table 1. Results of static and cyclic fatigue tests

	Static fatigue (x2)	Cyclic fatigue (x3)
Stress at failure	84 % of σ_R	36-42 % of σ_R
Strain at failure	ε_R	0.36 % of ε_R
Elastic modulus at failure	$E_f . v_f$	1.5 $E_f . v_f$
Number of AE sources	9500	$2.57.10^6$
Cumulated acoustic energy	$2.2.10^8$ (attoJ)	$6.4.10^{10}$ (attoJ)
matrix cracks spacing / matrix cracks spacing after tensile test	1	1.6

For both types of loading, stress at failure is lower than σ_R, nevertheless it is twice as high for static loading than for cyclic loading which means that cyclic loading has an effect on the material lifetime. Considering the strain at failure, the value is also lower for a cyclic loading than for a static loading. The evolution of this parameter differs in the two cases. For a static loading the evolution can be divided in two parts (Figure 5), it increases only during the first load of the stage due to matrix cracking until stage 5 ($0.42.\sigma_R$). From stage 6 ($0.48.\sigma_R$), the strain increases even when the load is constant because of debonding at the interfaces. This is in accordance with tensile test results since for the transition between parts I and II of the strain is around 18% of σ_R. For a cyclic loading, the material behaves in the same way for a low value of maximal stress (Figure 6). Nevertheless, maximal strain is increasing all along stage 4 ($0.36.\sigma_R$) and is still increasing during stage 5. The elastic modulus during those stages is decreasing whereas it only evolves during the first loading cycles within stage 0 ($0.12.\sigma_R$) to stage 3 ($0.30.\sigma_R$). Thus the cyclic loading has an effect on damage starting from stage 4, which is not the case for a static loading. In addition, the elastic modulus decreases greatly before ultimate failure

(Figure 8) while it tends to an asymptotic value for a static loading (Figure 7), and does not reach the value $E_f v_f$. Moreover, the mean distance between matrix cracks in the longitudinal strands of the samples shows that matrix cracking does not reach its saturation for a cyclic loading. This means that the material damages differently when a cyclic loading is applied. (It probably generates wear at the interfaces due to friction.)

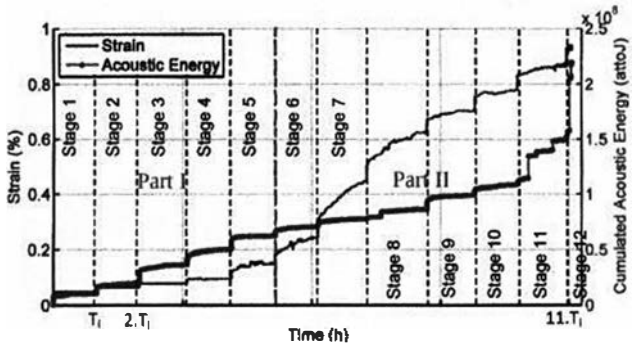

Figure 5. Strain & AE energy vs. time during a static fatigue test (stage 1: $0.18.\sigma_R$, stage 12: $0.84.\sigma_R$)

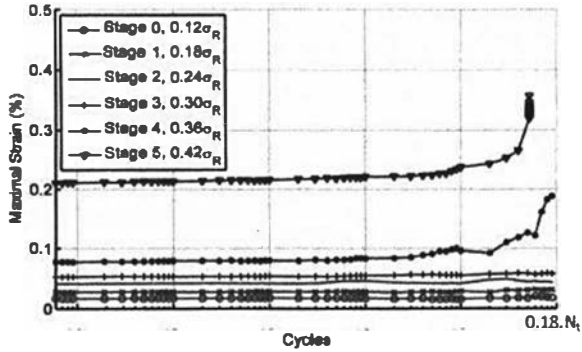

Figure 6. Maximal strain vs. number of cycles during each stage of a cyclic fatigue test (stage 0: $0.12.\sigma_R$, stage 5: $0.42.\sigma_R$)

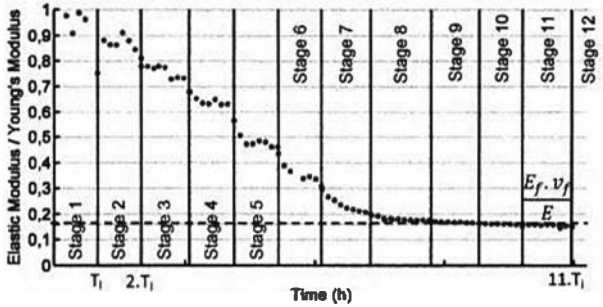

Figure 7. Elastic modulus vs. time during a static fatigue test (stage 1: $0.18.\sigma_R$, stage 12: $0.84.\sigma_R$)

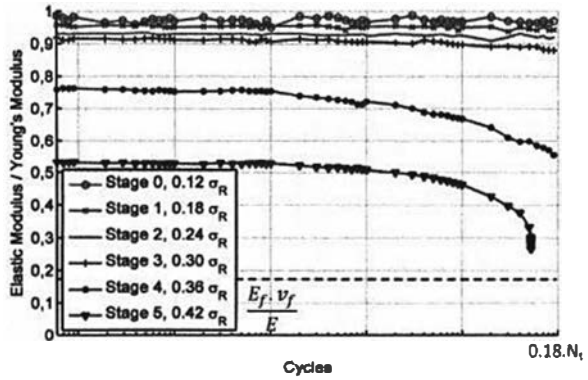

Figure 8. Elastic modulus vs. number of cycles during each stage of a cyclic fatigue test (stage 0: $0.12.\sigma_R$, stage 5: $0.42.\sigma_R$)

Acoustic Energy

The analysis of the evolution of acoustic energy during a tensile test shows that high energy signals are generated when matrix is cracking and at the end of the test when the whole load is carried by the fiber only, which is due to fiber breakages (Figure 4). Analyze of acoustic energy during fatigue tests shows different behaviors depending on the type of loading.

For a static loading, during each stage, the activity can be decomposed in 2 parts: AE generated during the loading part of the stage and AE generated when the load is constant. This makes possible to make out 2 phases during the whole test (Figure 5). Within stages 1 to 5 ($0.18.\sigma_R$ to $0.42.\sigma_R$), the acoustic energy is more significant during loading part than when the load is constant (twice as higher during the loading phase than during the constant load phase). It is the result of a large energy release when matrix is cracking whereas acoustic activity is weak at constant load where the material is not damaged. Starting from stage 6 ($0.48.\sigma_R$) the trend is reversed, constant load phases are more energy generating. This shows one more time that there

is a transition in the damage mode between stages 5 and 6 and loading higher than 48 % of σ_R for a static fatigue test has consequences on material damage.

During cyclic fatigue test, 3 parts clearly appear on the acoustic energy evolution (Figure 9). Part I which includes stage 0 to stage 2 ($0.12.\sigma_R$ to $0.24.\sigma_R$) is composed of approximately 9000 sources localized in the gauge section, whereas the average activity is 1 source per cycles in part II and III. This activity is generated mostly at the beginning of the stage, at maximal stress, which seems to be generated by matrix cracking. The important increase during part II shows that the material behavior is different when the load is cyclic already during stage 3 ($0.30.\sigma_R$). It is generated mostly for maximal stress, but activity appears as well during the unloading part of cycles, for a low stress. This acoustic activity may be generated by friction at the interfaces when matrix cracks are closing and opening. A third part appears at stage 5 ($0.42.\sigma_R$), which has the same average sources per cycles but a higher average energy per signals. By calculating the R_{ae} for static fatigue tests (Figure 10. a.), it can be seen that there are activity peaks for each load at the beginning of stages. In the case of cyclic loads (Figure 10. b.), it shows similar kind of evolution during stages 0 to 2 ($0.12.\sigma_R$ to $0.24.\sigma_R$), and then the curve oscillates around a mean value during stages 3 to 4 ($0.30.\sigma_R$ to $0.36.\sigma_R$), and is growing during stage 5 ($0.42.\sigma_R$),, which confirms presence of 3 different parts in the test, with different damage modes.

Furthermore even if the material does not seem to damage at stage 3 ($0.30.\sigma_R$),from a mechanical point of view, the different evolution of acoustic activity at that stage shows that there are already consequences of a cyclic load which is probably due to wear at interfaces which could reduce the material lifetime.

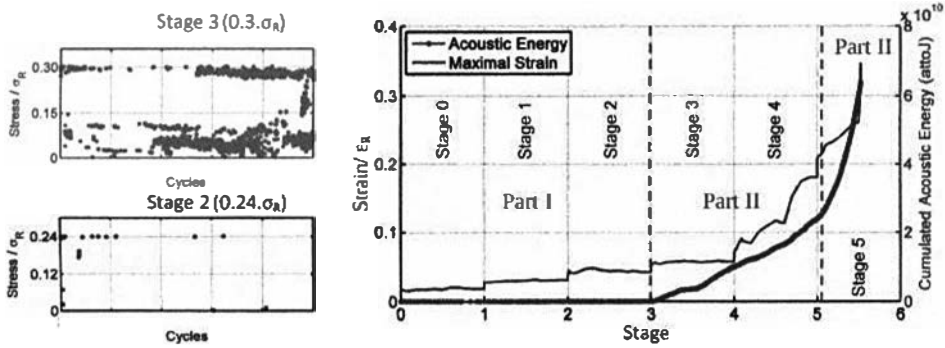

Figure 9. Maximal strain & AE energy vs. number of cycles during a cyclic fatigue test (stage 0: $0.12.\sigma_R$, stage 5: $0.42.\sigma_R$) and stress for localized signals with amplitude over 60 dB

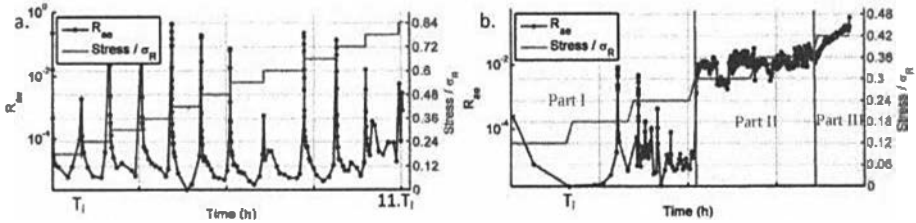

Figure 10. *Rae* vs. time during a. static fatigue test (N=100, n=90) - b. cyclic fatigue test (part I: N=100, n=90 – part II / III : N= 5000, n= 4900)

Sentry Function

In order to have a good understanding of the sentry function variations, it has first to be calculated for a tension test (Figure 11). The sentry function can be divided in 2 parts in this case. During the first part, the function value stabilizes around a mean value. It corresponds with matrix cracking in the material. The variations of the function can be explained by the large increase of acoustic energy created by this phenomenon which is balanced by the increase of strain energy. The function evolves in the same way for static fatigue test (Figure 12), until a strain of 0.18 % which corresponds to the transition between stages 5 and 6 ($0.38.\sigma_R$ and $0.42.\sigma_R$). The transition between parts I and II is due to a reduction of matrix cracking, which almost reaches its saturated value, and the strain increase caused by debonding at the interfaces. The fact that the function behaves in the same way for the cyclic fatigue (Figure 13) test between stages 0 and 2 ($0.12.\sigma_R$ and $0.24.\sigma_R$) is one more clue to confirm that the material is only damaged through matrix cracking.

During part II, the function is only directed by the evolution of strain. During tensile test, increase of the acoustic energy caused by fiber breakages at the end of the test is not high enough to modify the function variations. The situation is different for fatigue tests. In both cases a third part appears for an average time of 90 % of the total test duration. The function is then decreasing. The high energy signals which create this decrease are probably generated by fibers breakages since they are localized, for a static and a cyclic load, in the area where the specimen failed. It can be seen on Figure 12 and Figure 13 where the location of energizing signals which create the decrease of the function is presented.

The cyclic fatigue test shows an extra part (part I.b) where the function is decreasing significantly. This is caused by the large increase in acoustic energy described below, where the strain remains constant. It appears that cyclic loading generates different types of damage since the function does not show this type of variation for a static loading or a tensile test.

The variations of this function in different cases point out different levels of the damage of the material: matrix cracking and fibers breakages for fatigue tests. Furthermore it points out that a cyclic loading has more critical consequences than static loading when the maximal stress is higher than 36 % of σ_R.

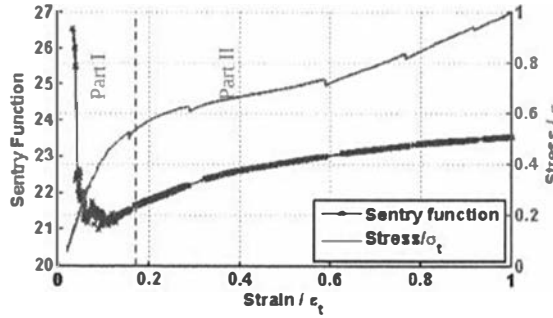

Figure 11. Sentry function & stress vs. strain for a tensile test (k= 5)

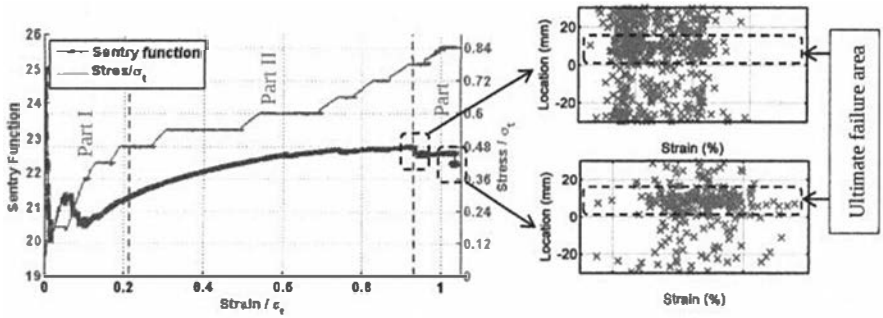

Figure 12. Sentry function for a static fatigue test (k = 10)

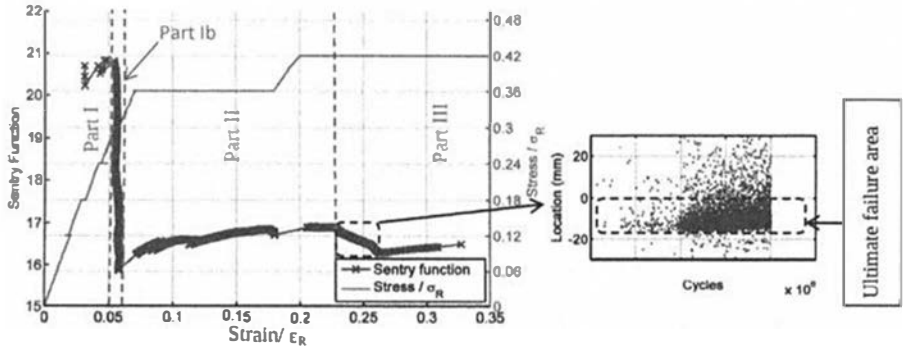

Figure 13. Sentry function for a cyclic fatigue test (k=1000)

CONCLUSION

Realization of fatigue tests with incremental loads makes possible to determine what level of stress can damage the material. Furthermore, comparison between static and cyclic tests shows that cyclic loading higher than 36 % of σ_R has consequences on damage and on material

lifetimes. In addition, the sentry function makes possible to link complementary data: mechanical and acoustic data. It demonstrates different phases in damage evolution for fatigue loadings (matrix cracking, fibers breakages) and gives clues on the behavior of the material under these kinds of loading. Even if precision has to be improved; the use of this tool is promising to create a real-time damage indicator.

ACKNOWLEDGEMENTS

The collaboration with Snecma and Herakles is gratefully acknowledged. This work was supported under the PRC Composites, French research project funded by DGAC, involving SAFRAN Group, ONERA and CNRS.

REFERENCES

[1] J. Lamon, CVI SiC/SiC composites NP. Bansal (Ed.), Handbook of ceramics composites, Springer, 2005.

[2]O. Loseille, J. Lamon, Prediction of lifetime in static fatigue at high temperatures for ceramic matrix composites, *J. Adv. Mat. Res.*, 112:129-40, 2010.

[3]GN. Morscher, Modal acoustic emission of damage accumulation in a woven SiC/SiC composite. *Compos Sci Technol*, 59 pp687--697, 1999.

[4]GN. Morscher, AL. Gyekenyesi, The velocity and attenuation of acoustic emission waves in SiC/SiC composites loaded in tension. *Compos Sci Tech-nol*, 62 pp 1171–1180, 2002.

[5]M. Moevus, N. Godin, M. R'mili, D. Rouby, P. Reynaud, G. Fantozzi And G. Farizy, Analysis of damage mechanisms and associated acoustic emission in two SiCf/[Si-BC] composites exhibiting different tensile behaviours. Part II: Unsupervised acoustic emission data clustering, *Composites Science and Technology* 68(6): 1258-1265, 2008.

[6]S. Momon, N. Godin, P. Reynaud, M. R'mili, And G. Fantozzi, Unsupervised and supervised classification of AE data collected during fatigue test on CMC at high temperature, *Composites Part A: Applied Science and Manufacturing*, 2011.

[7]E. Maillet, N. Godin, M. R'Mili, P. Reynaud, G. Fantozzi, J. Lamon, Damage monitoring and identification in SiC/SiC minicomposites using combined acousto-ultrasonics and acoustic emission, *Composites Part A*, 57 8–15, 2014.

[8]S. Momon, M. Moevus, M. R'mili, P. Reynaud, G. Fantozzi And G. Fayolle, Acoustic emission and lifetime prediction during static fatigue tests on ceramic-matrix-composite at high temperature under air, *Composites Part A: Applied Science and Manufacturing* 41(7): 913-918, 2010.

[9]E. Maillet, N. Godin, and M. R'mili, P. Reynaud, G. Fantozzi and J. Lamon. Real-time evaluation of energy attenuation: A novel approach to acoustic emission analysis for damage monitoring of ceramic matrix composites. *J Eur Ceram Soc*, 2014, http://dx.doi.org/10.1016/j.jeurceramsoc.2013.12.041

[10]E. Maillet, N. Godin, And M. R'mili, P. Reynaud, J. Lamon And G. Fantozzi, Analysis of Acoustic Emission energy release during static fatigue tests at intermediate temperatures on Ceramic Matrix Composites: Towards rupture time prediction, *Composites Science and Technology*, 72 pp 1001–1007, 2012.

[11]G. Minak, P. Morelli, And A. Zucchelli, Fatigue residual strength of circular laminate graphite–epoxy composite plates damaged by transverse load, *Composites Science and Technology*, vol. 69, no 9, p. 1358-1363. 2009.

[12]G. Minak, And A. Zucchelli, Damage evaluation and residual strength prediction of CFRP laminates by means of acoustic emission techniques, *Composite Materials Research Progress*. Nova Science Publishers, New York, pp 167-209. 2008.